Hindawi
International Journal of Energy Research
Volume 2023, Article ID 5547603, 21 pages
https://doi.org/10.1155/2023/5547603

WILEY | Hindawi

Research Article

Switched-Resistor Passive Balancing of Li-Ion Battery Pack and Estimation of Power Limits for Battery Management System

Sonu Kumar,[1] **S. Koteswara Rao**,[1] **Arvind R. Singh**,[2] **and Raj Naidoo**[2]

[1]*Department of Electronics and Communication Engineering, Koneru Lakshmaiah Education Foundation, Vaddeswaram, Guntur, Andhra Pradesh 522302, India*
[2]*Department of Electrical, Electronic and Computer Engineering, University of Pretoria, Pretoria, South Africa*

Correspondence should be addressed to Arvind R. Singh; u17410411@tuks.co.za

Received 21 March 2023; Revised 13 May 2023; Accepted 15 May 2023; Published 17 June 2023

Academic Editor: Ahmad Azmin Mohamad

The battery pack performance and expected lifespan are crucial in electric vehicle applications. Balancing the charge on a battery pack connected in series and parallel is crucial due to manufacturing discrepancies and distinct performance of each cell in a standard battery pack. In this paper, a switched-resistor passive balancing-based method is proposed for balancing cells in a battery management system (BMS). The value of the available voltage at the battery cell terminals is balanced using resistors in an electrical circuit, and the excess voltage is eliminated. The cell balancing outcome demonstrates that the electrical circuit can maintain an even voltage across each cell. The procedure of balancing involves individually adjusting each cell's level of charge. Passive balancing releases energy as heat by draining charge from cells that have too much charge. A passive cell balancer is a cost-effective solution and easy to install, but due to thermal loss from a resistor, it has a low energy efficiency for cell balancing and necessitates a lengthy balancing process. This passive cell balancer is an effective and reliable method for low-power devices and portable applications such as electrical vehicles. The power limits during charging and discharging are estimated using the bisection method.

1. Introduction

The price of petroleum and its effects on the environment have recently sparked a surge in interest in electric vehicles in the transportation industry. The IC engine vehicles are responsible for the increase in fuel prices and environmental effects like air pollution. If EVs are used, compared to conventional energy sources, the amount of air pollution can be reduced by three times. For battery-operated electric vehicles, operational efficiency has grown above 80%, resulting in a decrease in the cost of energy used [1]. When compared to the ordinary IC combustion engine's 20% efficiency, the energy efficiency is also raised to higher rates of 60 to 80% [2]. The range of electric vehicles is increasing as the drive trains become less expensive, more rigid, and no emissions of hazardous gases [3, 4].

Electric vehicles become a new medium of cheap, reliable, and safe transportation for the environment, which can overcome the threat of energy crisis [5]. The general consensus is that electric vehicles (EV) are a crucial transitional technology for environmentally friendly and energy-efficient transportation [6]. It has great benefits such a small volume, a huge capacity, less weight, and increased safety [7–9]. Battery as a primary power source for electric vehicles becomes a crucial component. Due to chemical reasons, batteries must be protected against overcharging in order to avoid an irreversible chemical reaction that would damage the battery's internal cell structure and result in lower battery performance and storage capacity [10]. The battery management system (BMS) includes a wide range of capabilities to assist the user in managing the battery and avoiding charging failure [11]. Among the services a BMS offers are battery optimisation, protection, and monitoring. The cell balancing method [12–14] is an integral part of BMS and serves a number of critical purposes. Battery balancing is part of an optimisation problem. A comprehensive BMS has governed charging with constant current constant voltage (CCCV) to guarantee that all the cells get fully charged and all cells are balanced,

i.e., have same voltage level and safety features included into the battery pack to shield the driver and passengers from harm in the case of a malfunction [15, 16].

The complicated characteristics of power batteries, including their high capacity, high power, extensive temperature change, and challenging operating circumstances, must be handled by BMS. When a power battery is mishandled, it may experience extreme conditions including overcharging, overdischarging, and overheating, which can lead to subsequent fires or even explosions in some extreme cases. To keep the battery in a safe state and to balance the capacity between the battery cells, the cell balancing circuit is crucial. State of health (SOH) refers to the battery's overall condition and its ability to deliver the desired results in contrast to its initial state. When the battery reaches a certain threshold of degradation, the SOH indicator alerts the user that maintenance or a battery replacement is needed in order to lower the likelihood of battery failure [17]. Algorithms for voltage balancing and state of charge balancing are the two most often utilised algorithms for balancing cells. Voltage balancing has been the subject of extensive investigation [5].

In order to efficiently identify outliers (i.e., unbalanced cells), the algorithm selects the typical properties of battery cells [18, 19]. The abnormal cells are balanced by a passive balancing circuit after the exact classification of normal and abnormal cells has been obtained using the clustering method. An accurate outlier detection method may identify aberrant battery cells and enhance the performance of the battery pack by boosting useable energy and increasing lifetime. Typically, the cell chemicals, initial charge capacities, and exterior impacts of each battery pack cell vary. Additionally, the battery pack's series-connected cells are often charged and discharged in different energy storage systems. Therefore, there may be an uneven state of charge in the battery cells as a result of the variations in charge-discharge speed and lifetime [20]. Changes in voltage and cell's capacity in series connection in a pack are caused by the variances in charging and discharging rates in these unbalanced cells. These changes in the battery pack are the primary cause of decreased cell capacity and shorter battery life. An auxiliary cell balancing circuit should be utilised in BMS to correct this energy imbalance in the cells.

These variations can also be caused by the charge and discharge cycles of the cell and operating temperature. The variations cause an imbalance in the cells during charge and discharge and lead to issues such as (1) undercharging occurs when one or more cells in the string are charged below their maximum capacity. This reduces the overall capacity of the battery pack. (2) Overcharging occurs when the cells are charged above their capacity. It is a dangerous situation, and sometimes there can be a thermal runaway and an explosion. (3) Under discharging occurs when one or more cells in the battery pack reach their lower threshold while the other cells still have considerable capacity left in them. The battery management system misjudges the situation and assumes the pack to be completely discharged. (4) Over discharging occurs when the cell is discharged below its lower threshold. It can permanently damage the electrodes of the cell, and sometimes even a short circuit might occur. To avoid the above-mentioned conditions, it is necessary to implement cell balancing mechanisms that can equalize the charge contained in the cells.

The process of altering how much charge is present in each individual cell is known as balancing. Balance can be achieved in two primary ways: passive balancing removes charge from cells with excess charge and releases it as heat and active balancing which shifts charge from "high cells" to "low cells" in an effort to preserve energy in the battery pack.

Causes of imbalance can be listed as (a) imbalance results from anything that could lead to a SOC divergence between two cells, (b) cells with different Coulombic efficiencies, and (c) cells are given the same initial conditions (the same $z(0)$, the same Q, and the same i_{net}). However, as a result of varying efficiency η, cell SOCs differ while being charged. Another factor that might contribute to imbalance is when cell's net currents differ from one another.

Coulombic efficiency can be given as

$$z(t) = z(0) - \frac{1}{Q}\int_0^t \eta(\tau) i_{\text{net}}(\tau) d\tau. \tag{1}$$

Current equation can be represented by

$$i_{\text{net}}(t) = i_{\text{app}}(t) + i_{\text{self-discharge}}(t) + i_{\text{leakage}}(t), \tag{2}$$

where $i_{\text{app}}(t)$ is the current being drawn from the battery pack during application, $i_{\text{self-discharge}}(t)$ is the rate at which individual cells discharge their stored energy, and $i_{\text{leakage}}(t)$ is the current used to run the BMS circuit.

Various cells may have varying self-discharge rates, resulting in different $i_{\text{net}}(t)$. Varying cells may experience different leakage currents, which can change $i_{\text{net}}(t)$.

Figure 1 represents good and bad cell w.r.t. SOC variations. Unbalance occurs when cells draw a net current that is different from one another. A pack temperature gradient can exacerbate the issue because self-discharge rates, electronic performance, and Coulombic efficiency are all temperature-dependent.

A balanced battery pack has cells that are all at the same state of charge (SOC) at some point in its cycle [21]. What real-time standard should be used to choose which cells to balance? (a) Which balancer circuits should ever be "turned on"? (b) Until ΔSOC at the balancing set point is tiny, we might decide to balance using SOC estimates. However, it can balance wrong cells if SOC calculations are bad. (c) Another option for balancing, particularly when employing quick active balancing, is to rely on voltage measurements (until Δv is minimal). Voltage is a poor predictor of SOC, but it is simpler. Wasteful since it frequently balances the "wrong" cells, (d) even balancing based on total energy available is an option. It ensures that the battery pack's potential energy is used to the fullest extent, prior to reaching a design limit, often for the minimum cell voltage. Battery SOC (and consequently voltage) can be increased by allowing current to flow via low to

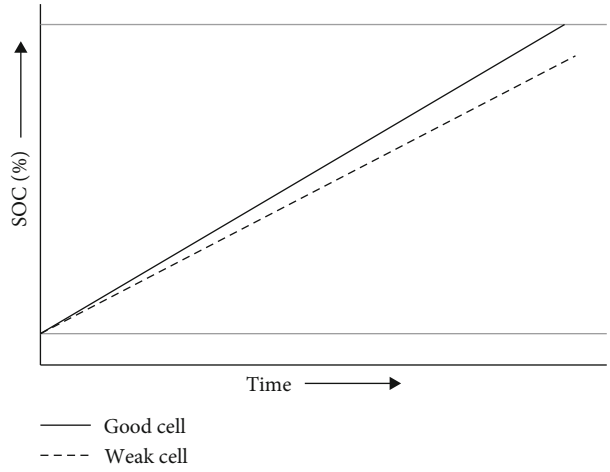

Figure 1: Representation of good and bad cell in a battery pack.

high resistance loads. For each cell, a precise cell model and state estimation are required.

Design for balance activities can be done considering the following things. When it should be balanced is another problem that must be fixed. (a) Continuously: required for HEV; required if quick active balancing is performed to maximise the amount of power and energy in the pack that is available. Being accurate with SOC estimates makes doing it right harder. (b) On charge only: applicable to EV, PHEV, and E-REV. Increases range: only when plugged in does the charge disappear. However, longer charging durations are necessary to enable full balance. (c) Predictive: predict the location of the charge's end point. Even when it is not immediately clear that balancing is required, it balances proactively.

Active balancing solutions save an additional 4.15 percent of energy per charge/discharge cycle for the total battery pack, as shown by the authors' experimental setup results from four separate case studies [22]. Their large energy storage capacity [23] makes them more unstable than other batteries like lead-acid batteries, and they need to be closely monitored to make sure they stay within their safe working limits. According to the authors' documentation in [24], some cells in these battery packs have a different state of charge (SOC) than others. This is because temperature, leakage current, and self-discharge rates will become imbalanced after being subjected to multiple charge/discharge cycles. This charge imbalance makes subsequent charge/discharge cycles more challenging and reduces the battery's total capacity. Due to differences in production and temperature, internal impedance, and self-discharge rates, cells in series strings will always be mismatched [25]. As the performance of a battery is dictated by the weakest cell in the chain, a mismatch results in a loss of capacity or power during charge or discharge mode. Improper cell balancing shortens the battery's lifespan and increases the risk of an explosion. A supercapacitor [26] is charged to act as a replacement for the cell with the highest state of charge (SOC) in the balancing circuit during vehicle regeneration. A switched-resistor balancing circuit is modelled using the theory of switched systems [27]. Then, the particle swarm optimisation method is fused with the cell balancing design. In [28], the authors provide a comprehensive overview of state-of-the-art approaches to cell balancing in low-voltage environments. Everything from the size and cost of the circuit to the needed speed of balancing and the complexity of the controls is considered. Passive balancing is an easy-to-implement and low-cost cell bypass strategy. Cell-to-cell balancing processes can considerably enhance energy efficiency; nevertheless, they have higher system costs and control complexity than cell bypass balancers. SOC estimate increases processing complexity [29] when voltage-based balancing is used. We present a simple method for SOC estimation using a generic extended state observer, which does not rely on any sensors in use at the moment and may thus materialise the system's resilience in the face of disruption.

In [24], the authors of the li-ion battery pack present an overview of converter-based cell balancing topologies. Approaches that use energy-efficient DC-DC converters to optimise cell balancing in medical devices are discussed. These approaches take into account circuit design, balancing time, implementation ease, and cost. This research paper [30] examines equalization circuits that use capacitors, inductors, and transformers. It provides a comprehensive comparison and shows how researchers have enhanced and adjusted these fundamental circuits. The purpose of this function may be to create [31], with battery thermal performance and cell SOH as inputs. A supercapacitor can be used to power the vehicle's traction motors and reduce the length of time that low state of charge (SOH) or high-temperature (Tc) cells are in use, hence extending the lifespan of the batteries. The audit will look at things like voltage balancing, current protection, cell voltage monitoring, and temperature [32] regulation. In this investigation, we introduce the equalization circuit construction and equalization technique [33], and we explore the characteristics of many equalization approaches. Some general factors, such as equilibrium and component efficiency, are used to evaluate various voltage balancing circuit topologies [34]. Because of inherent and environmental differences between supercapacitor cells and the need for series connections, the entire pack must undergo voltage equalization [35]. A comparison research takes into account things like price, time, efficiency, speed, size, modularity, and control [36]. In order to keep the battery charged consistently, the authors of [36] suggest employing an equilibrium technique based on an artificial potential field. By apportioning the charging current in an even fashion, the battery's charge can be brought to an even state. Although equalizers based on capacitors are convenient and inexpensive, they pose a risk to cells because of the surge currents they generate. Inductors allow for rapid regulation of current and balance when used in equalizers. They are expensive, bulky, and difficult to install and experience magnetization losses and saturation problems. Equalizers based on converters regulate both the incoming cell current and the outgoing cell current [37]. As far as possible, you should try to minimize the time spent charging and maximise the period between charges. This cannot happen until all the cells in the pack are in sync with one another.

Table 1: Comparison of accuracy of cell balancing techniques.

Sr. no.	Method	Accuracy	References
1	FLC	Improve the equalization time and efficiency by 49% and 48%, respectively	[47]
2	FLC	Minimizes SOC deviation and equalization duration by 18.5% and 23%	[48]
3	Neuro-fuzzy	Obtained a learning accuracy error of 1.8×10^{-5}	[49]
4	MPC	Balancing terminates when SOC difference is 2%	[50]
5.	MPC	Achieves 93% efficiency in balancing	[51]
6.	GA	GA scheme reduces equalization time by 1002.5 sec, and GA scheme improves energy efficiency 93.1%	[52]
7.	PSO	Achieves the maximum SOC gap within 2%. Improves the capacity by 13.2%	[53]
8.	ACO	Obtains total energy loss up to 1.53 in entire balancing process	[54]

The discrepancies between individual cells in large lithium-ion battery packs make recycling them difficult [38]. A less efficient and perhaps dangerous charging process results from an unbalanced pack caused by these differences. The RC mode of operation greatly decreased the current that was transferred between neighbouring cells [39]. Since this equalizer does not rely on capacitors, it can be used in battery banks that span a wide voltage range [40]. Each cell's voltage and charge is brought back to their normal values by a virtual force function [41] generated by the artificial potential field. A feedback control law evenly distributes the battery charge current to quickly achieve balance among the batteries. The coupled inductor's magnetizing inductance is preserved during construction [42]. An industry-standard balancing circuit with n switches was designed to provide uniformity throughout a battery pack's cells. In comparison to the standard cuck converter-based balancing, the voltage loss is less when two MOSFETs per cell are used as the switch. We also provide a method for determining the optimum frequency at which a balanced active cell can function [43], as well as a control circuit to maintain that frequency. When such optimally scaled active cell balancing designs are run by choosing the best frequency, energy can be dissipated by around 49% less than it would be using the intuitive method of picking parts with the lowest parasitic resistances, as shown by the results of case studies. For the equalization of all cells of supercapacitors connected in series, the balancing procedures need to have a fast equalization speed [44], high efficiency and reliability, cheap cost, easy control, and a simple structure. Passive and active balancing strategies can be distinguished. If a battery cell is replaced but does not have the same charge as the others, the battery will not be destroyed, but it will take more time to equalize, as stated by the authors in [45]. To finish out the monitoring infrastructure, a new Bluetooth-based smart-monitoring system and a mobile application built with "MIT app inventor 2" track the voltage levels of individual cells. Each cell's potential in a series-connected battery pack should stay the same under ideal charging and discharging conditions [46]. Possible mismatch between series-connected cells affects charging and discharging of a battery pack.

The comparison of cell balancing using different methods is shown in Table 1.

The structure or the full manuscript is described here. Section 2 of the manuscript represents cell balancing techniques, with details about passive cell balancing techniques. Section 3 represents power limit estimation during charging and discharging process, Section 4 describes about methodology used for conducting this research activity, Section 5 represents the result obtained from this research activity, and Section 6 represents the concluding remarks.

2. Cell Balancing Techniques

In the literature, various cell balancing algorithms have been presented. Methods for balancing cells are often divided into two categories: passive circuits and active circuits. By utilising more energy cells than others, a passive cell balancing method uses resistors to balance the cell energy of a battery pack. Despite being simple to design, this passive cell balancing circuit typically has a low energy transfer efficiency due to energy losses brought on by heat dissipation from the resistors. On the other approach, an active cell balancing circuit uses a power electronic interface to convert higher cell energy to lower cell energy. This active cell balancer is more effective than a passive cell balancer, but because each cell must be coupled to a separate power electronic interface, its control algorithm may be complicated and its production costs high [55].

In a cell balancing system, a wide range of general electronic techniques may be applied. For Li-ion batteries, several cell balancing techniques have been devised [56, 57]. Based on cell voltage and SOC, it can be divided into passive and active cell balancing approaches [58, 59]. Figure 2 lists the topologies that are most typical.

Through the use of resistor components, the passive equalizing procedures remove the excess charge from fully energised cells, making all the cells with a charge that is identical to that of the lowest cell [60]. Passive balancing is suitable for lower power applications such as electrical vehicles [12]. In active balancing, cells transfer discharge from high- to low-energy cells [61–63]. The intricate circuitry used in this method raises the cost of the entire system. Active cell balancing is therefore appropriate for higher power application [64–67].

2.1. Passive Cell Balancing. To dissipate extra energy from the high-voltage cells in a series string, passive equalization relies on resistance [68]. Due to the inexpensive components and straightforward control mechanisms, this type of

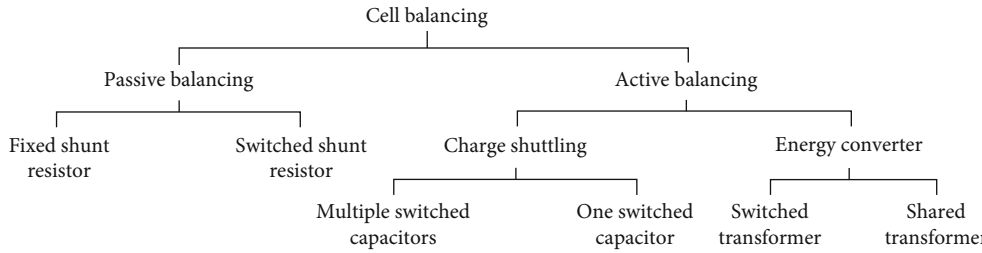

Figure 2: Cell balancing methods.

equalization is most used in industry [69]. Till all the cells come in equilibrium with the remainder of the string, energy is dissipated as heat [70]. Due to power losses and thermal management, the equalization current must be kept at a very low level, which results in longer balancing time [71]. Passive cell balancing techniques are of two types: (1) fixed shunt resistor and (2) switched shunt resistor. Both are explained in below sections.

2.1.1. Fixed Shunt Resistor: Passive Balancing. For passive balancing systems, the simplest electronic designs are used. In general, each cell has a resistor connected in parallel with it that is utilised to remove charge. The energy that is taken out of the cell is released as heat. The fixed shunt resistor design is very simple compared with other designs. Figure 3 depicts a shunt resistor balancing circuit, where R_1, R_2, …, R_n are resistances and BC_1, BC_2, …, BC_n are individual cells.

According to the theory, high-voltage cells will self-discharge more quickly than low-voltage cells due to their higher balancing current. However, keep in mind that even if the pack is evenly distributed, the circuit is always losing charge. If the voltage goes down a certain level, a variant of the device utilises the Zener diodes to switch off balancing. This fixed shunt resistor passive balancing circuit with the Zener diode is shown in Figure 4, in which R_1, R_2, R_3, …, R_n are resistances; ZD_1, ZD_2, …, ZD_n are the Zener diodes; and BC_1, BC_2, …, BC_n are individual cells.

The Zener voltages were selected to match a 100% SOC set point. In the case of a lead-acid battery, that voltage is 2.20 volts. The resistor circuit is turned on, when the voltage rises beyond the Zener set point, which causes the charge to be slowly drained away until the cell's voltage falls beneath the Zener set point. It should be noted that this design is applicable to lead-acid and nickel-based chemistries only; lithium-ion chemistries are not supported by this design.

2.2. Switched Shunt Resistor: Passive Balancing. The Zener diode can be changed out for a BMS-controlled switch in order to adapt the above concept to lithium-ion chemistries. This switch is some kind of transistor circuit as shown in Figure 5. In Figure 5, R_1, R_2, …, R_n are resistances; S_1, S_2, …, S_n are switches; and BC_1, BC_2, …, BC_n are individual cells.

This design is more complex due to the electronics needed to operate the transistor, but the balancing method is far more flexible. When a cell has too much charge, the BMS closes switches, enabling the cell to drain. The circuitry

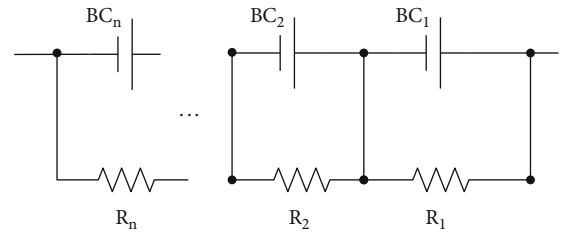

Figure 3: Fixed shunt resistor passive balancing circuit.

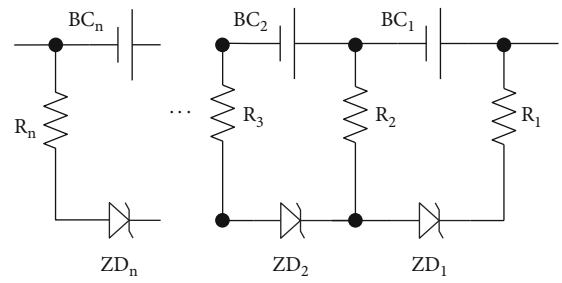

Figure 4: Fixed shunt resistor passive balancing circuit with the Zener diode.

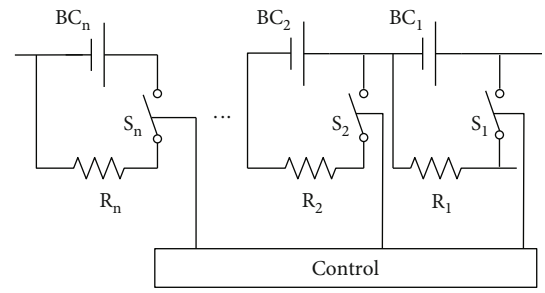

Figure 5: Switched shunt resistor passive balancing circuit.

to control either an internal transistor switch or a battery stack is incorporated into current battery stack monitoring or an external transistor switch, so the increased complexity is not as significant an issue as it formerly was (for faster balancing). When compared to active balancing systems, the main benefit of any of these passive balancing methods is the simplicity (and hence reduced cost) of the circuits involved.

Shortcoming of this technique are as follows: (1) Energy that may be used for other purposes is wasted as heat as a result of this practise. (2) In a balance-at-top design, after a weak cell is fully discharged, energy is still present in the cell

that might be used by an active balancing system. (3) Heat is produced. The energy lost as heat is given as

$$P \approx V_{\text{nom}} \times I_{\text{balance}}. \tag{3}$$

More heat is produced in rapid balancing. The balancing transistors and resistors are typically required to have high current ratings and high wattage requirements, respectively. The amount of heat produced during balancing may be comparable to the heat produced during typical cell operation. Managing heat is expensive that may need to do more cooling as a result. Comparing the life of a battery pack to one with an active balancing design, it may be shorter. The weakest cell in the pack decides whether the pack will survive. The pack can achieve a homogeneous end-of-life configuration by using strong cells to support weak cells through active balancing.

3. Power Limit Estimation

Power limit specifies how quickly we may add or remove energy from pack without disobeying a set of design constraints. It has been presumed that the cell terminal voltage is the main design limitation. A current research topic searches to use physics-based models and power limit calculations to compute limits determined not by terminal voltage but by gradual damage. Predictive computations for the power limit are required. It is necessary to indicate the maximum constant discharge/charge power levels that can be considered "safe" over a time horizon of ΔT.

The power limits can be addressed for three things: (1) discharge power, (2) charge power, and (3) both discharge and charge powers. Estimating the maximum discharge power that can be kept constant for ΔT without exceeding preestablished design constraints for cell voltage, SOC, maximum design power or current, depending on how the battery is performing right now. Power when charging and discharging, where (1) and (2) can be coupled arbitrarily, can have different values for ΔT.

Limits also depend on the temperature and other aspects of the operating state of the battery pack at the time. Partnership for new generation vehicles (PNGV) described hybrid pulse power characterization (HPPC) technique for power limit estimation. In order to enforce constraints on cell terminal voltage, power is calculated. This power is predictive over the following ΔT and updates more frequently than once every ΔT. A simplified cell model is given in Figure 6.

The current can be expressed as

$$i(t) = \frac{\text{OCV}(z(t)) - v(t)}{R}. \tag{4}$$

To compute power limit, assume only that maintaining a terminal voltage between $v_{\min}$ and $v_{\max}$ is of interest to us. Calculate maximum discharge current as constrained

$$i_{\max,n}^{\text{dis,volt}} = \frac{\text{OCV}(Z_n(t)) - v_{\min}}{R_{\text{dis},\Delta T}}. \tag{5}$$

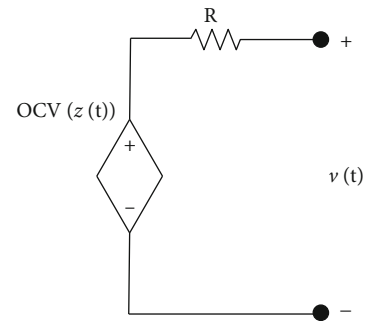

Figure 6: Simplified cell model.

Pack discharge power is then calculated as

$$P_{\max}^{\text{dis}} = N_s N_p v_{\min} \min_n \left(i_{\max,n}^{\text{dis,volt}} \right). \tag{6}$$

Set $R = R_{\text{chg}}$, T, and clamp $v(t) = \text{v}_{\max}$ for the charging power in equation (4).

Conventionally, charge current is supposed to have a negative sign and a signed minimum value for a maximum current.

$$i_{\min,n}^{\text{chg,volt}} = \frac{\text{OCV}(z_n(t)) - v_{\max}}{R_{\text{chg},\Delta T}}. \tag{7}$$

Pack charge power is then calculated as

$$P_{\min}^{\text{chg}} = N_s N_p v_{\max} \max_n \left(i_{\min,n}^{\text{chg,volt}} \right). \tag{8}$$

Hence, it can be said that HPPC power limit estimation method first collects current–voltage pulse data from cells and then calculates discharge/charge resistances $R_{\text{dis},\Delta T}$ and $R_{\text{chg},\Delta T}$. Using simplified cell model, it clamps terminal voltage to either $v_{\max}$ or $v_{\min}$ and uses pulse resistances to compute maximum-magnitude current. Then, it multiplies current by voltage to make estimate of power limits.

Similarly, limits based on SOC, max current, and power can also be obtained. If we have design limits such that $z_{\min} \le z_n(t) \le z_{\max}$, to impose these constraints, we can compute current for each cell in the pack. Current limitations are determined via simple mathematics using the SOC of each cell.

$$\begin{aligned} i_{\max,n}^{\text{dis,SOC}} &= \frac{z_n(t) - z_{\min}}{\Delta T/Q}, \\ i_{\min,n}^{\text{chg,SOC}} &= \frac{z_n(t) - z_{\max}}{\eta \Delta T/Q}. \end{aligned} \tag{9}$$

Power estimates can be made more conservative by using side information on SOC estimation uncertainty, such as data from xKF. This serves as (assuming here that we desire to use a $3\sigma_z$ confidence interval)

$$i_{\max,n}^{\text{dis,SOC}} = \frac{(z_n(t) - 3\sigma_{z,n}) - z_{\min}}{\Delta T/Q},$$
$$i_{\min,n}^{\text{chg,SOC}} = \frac{(z_n(t) - 3\sigma_{z,n}) - z_{\max}}{\eta \Delta T/Q}. \tag{10}$$

So, even if estimate of z_n is inaccurate, future SOC will not violate limits if estimate is within $\pm 3\sigma$ bounds.

Pack discharge currents with all restrictions in place are computed as soon as all cell current limits have been determined

$$i_{\max}^{\text{dis}} = N_p \min\left(i_{\max}, \min_n i_{\max,n}^{\text{dis,SOC}} \min_n i_{\max,n}^{\text{dis,volt}}\right). \tag{11}$$

We are finding the value of current closest to zero among all of the limiting currents based on electronics, future SOCs, and future voltages. Recalling that charge current has negative sign, "max" must be used to compute the value of current closest to zero.

$$i_{\min}^{\text{chg}} = N_p \max\left(i_{\min}, \max_n i_{\min,n}^{\text{chg,SOC}} \max_n i_{\min,n}^{\text{chg,volt}}\right). \tag{12}$$

Pack power is the total cell power calculated at the highest allowable current and expected future voltage.

$$P_{\min}^{\text{chg}} = \max\left(N_s p_{\min}, \sum_{n=1}^{N_s} i_{\min}^{\text{chg}} v_n(t + \Delta T)\right),$$
$$P_{\min}^{\text{chg}} \approx \max\left(N_s p_{\min}, \sum_{n=1}^{N_s} i_{\min}^{\text{chg}}\left(\text{OCV}\left(z_n(t) - i_{\min}^{\text{chg}} \frac{\eta \Delta T}{N_p Q}\right) - i_{\min}^{\text{chg}} \frac{R_{\text{chg}} \Delta T}{N_p}\right)\right),$$
$$P_{\max}^{\text{dis}} = \min\left(N_s p_{\max}, \sum_{n=1}^{N_s} i_{\max}^{\text{dis}} v_n(t + \Delta T)\right),$$
$$P_{\max}^{\text{dis}} \approx \min\left(N_s p_{\max}, \sum_{n=1}^{N_s} i_{\max}^{\text{dis}}\left(\text{OCV}\left(z_n(t) - i_{\max}^{\text{dis}} \frac{\Delta T}{N_p Q}\right) - i_{\max}^{\text{dis}} \frac{R_{\text{dis}} \Delta T}{N_p}\right)\right). \tag{13}$$

Hence, it can be said that we can compute power additionally based on future SOC limits, electronics current limits, and load power limits. Additionally, we can use confidence interval on SOC from xKF (Kalman filtering) to produce conservative estimate of available power.

We can use Octave code to compute HPPC limits. We now compute "truth" power limits using exact SOC from carefully calibrated lab tests. We can compute more realistic power limits using SOC estimate and bounds produced by sigma point Kalman filter (SPKF). SPKF method is more conservative because it uses bounds.

This improved HPPC technique still has its limitations. The utilised cell model is too simple to produce accurate findings. Overly optimistic or pessimistic results might be produced, either creating a risk for safety or battery health or using batteries inefficiently. Additionally, HPPC assumes the untrue starting equilibrium condition. As a result, we typically reduce the HPPC estimations by a trust factor. Better power prediction can be achieved by combining the most potent algorithm possible for using the cell model and a better cell model.

Now assume more accurate model in state-space form

$$x_n[k+1] = f(x_n[k], u_n[k]),$$
$$v_n[k] = h(x_n[k], u_n[k]). \tag{14}$$

Also, assume ΔT seconds is exactly $k_{\Delta T}$ sample time duration. After that, model can be used to estimate voltage ΔT seconds into future by

$$v_n[k + k_{\Delta T}] = h(x_n[k + k_{\Delta T}], u_n[k + k_{\Delta T}], \tag{15}$$

where $x_n[k + k_{\Delta T}]$ was found by simulating state equation for $k_{\Delta T}$ time samples. Assume that cell input remains constant from time index k to $k + k_{\Delta T}$, and denote it simply as u_n.

A special case is when the state equation is linear, when

$$x_n[k+1] = Ax_n[k] + Bu_n[k], \tag{16}$$

where A and B are constant matrices.

Charge power is then computed as

$$P_{\min}^{\text{chg}} = N_p \sum_{n=1}^{N_s} i_{\min}^{\text{chg}} v_n(t + \Delta T) = N_p \sum_{n=1}^{N_s} i_{\min}^{\text{chg}} h(x_n[k + k_{\Delta T}], u_n), \tag{17}$$

with u_n containing $i_{\min}^{\text{chg}}$ as its value for current.

Discharge power is computed as

$$P_{\max}^{\text{dis}} = N_p \sum_{n=1}^{N_s} i_{\max}^{\text{dis}} v_n(t + \Delta T) = N_p \sum_{n=1}^{N_s} i_{\max}^{\text{dis}} h(x_n[k + k_{\Delta T}], u_n), \tag{18}$$

with u_n containing $i_{\max}^{\text{dis}}$ as its value for current.

3.1. Bisection Search. To use full cell model to find $i_{\max,n}^{\text{dis,volt}}$, or seek u_n to solve

$$0 = h(x_n[k + k_{\Delta T}], u_n) - v_{\min}. \tag{19}$$

To use full cell model to find $i_{\min,n}^{\text{chg,volt}}$, or seek u_n to solve

$$0 = h(x_n[k + k_{\Delta T}], u_n) - v_{\max}. \tag{20}$$

Locating the root of a nonlinear equation is a problem that must be addressed. When it is known beforehand that at least one root lies between values x_1 root x_2, the bisection search method searches for a root of $h(x)$ (value of x such that $h(x) = 0$). The bisection algorithm assesses the function at the middle point $x_{\text{mid}} = (x_1 + x_2)/2$ for each iteration. To maintain the various signs on $h(x_1)$ and h, either x_1 or x_2 is replaced by x_{mid} depending on the evaluation's sign (x_2). This computational step reduces the uncertainty of the root position by half. Bisection iteration is repeated until interval

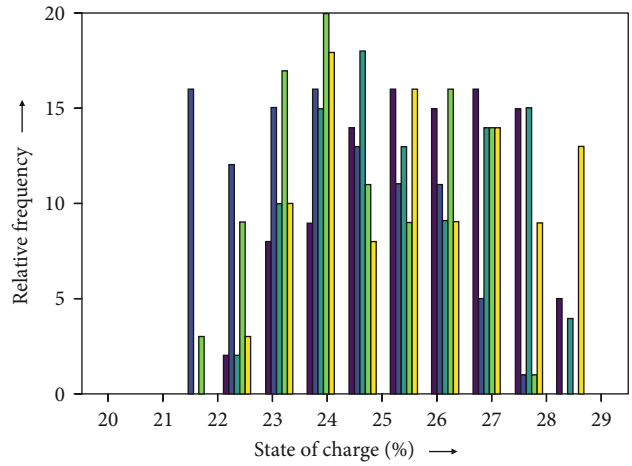

Figure 7: Individual SOC distribution after 20 cycles.

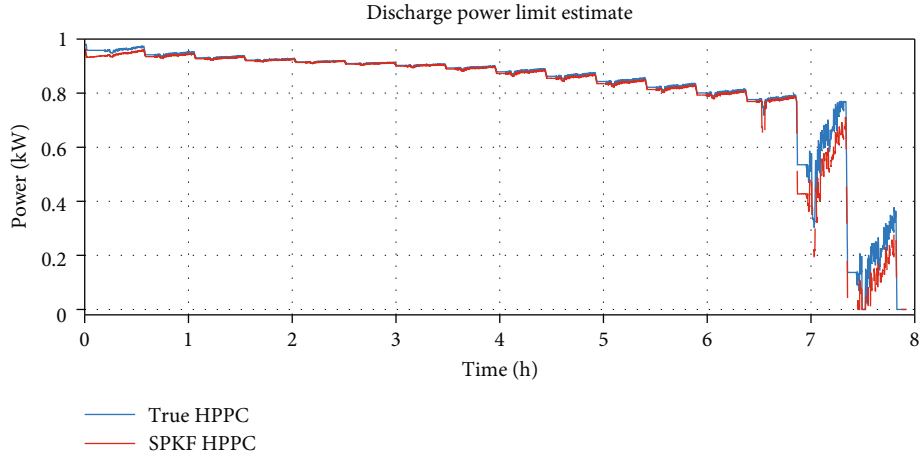

Figure 8: Discharge power limit estimation using HPPC and SPKF HPPC.

between x_1 and x_2 as small as desired: if ε is needed, precision and algorithm require at most $[\log_2(|x_2 - x_1|/\varepsilon)]$ iterations.

4. Methodology

In this study, the cell balancing for the battery pack was carried out using switched-resistor passive balancing technique. A battery pack having 100 cells used in an electric vehicle was chosen for this study. Once the vehicle moves around 5000 km, the battery cell individual SOC (%) was examined. It was found that the individual SOC (%) values for different cells are different, that means battery pack is unbalanced. Then, resistors along with the switching circuits were employed to balance the battery pack. Cells are balanced whenever their terminal voltage is more than 2 mV greater than the lowest terminal voltage of all 100 cells in the battery pack. Different values for resistors were used for balancing the same pack to know how much time it takes for balancing and how much power gets wasted in the balancing.

It was being attempted to minimize the power wastes in individual cells as well as for the entire battery pack. Also, the total time required for the balancing of the battery pack is considered. It was being attempted to balance the pack in a reasonably less time. Balancing resistance values from 5 Ω to 200 Ω were used for balancing. The balancing resistance values were fine-tuned to get the best results within acceptable values, for user's convenience. The cell balancing was carried out through simulation studies, carried out in Jupyter Notebook using Octave codes. Current variation and cell voltage variation, solid surface concentration at electrodes, solid potential voltage, electrolyte concentration, electrolyte potential, and flux variations were studied at negative and positive electrodes.

The power limit estimation was performed while the battery pack is being charged and discharged with the help of hybrid pulse power characterization technique, sigma point Kalman filtering, and bisection method. The SOC values were estimated using sigma point Kalman filtering. Using terminal voltage $V_{\min}$ and $V_{\max}$, discharge power limit was calculated. Octave codes were used to compute HPPC limits. Similarly, charging limit was calculated. The bisection search was repeated, till the interval between both roots became smaller as per the requirement.

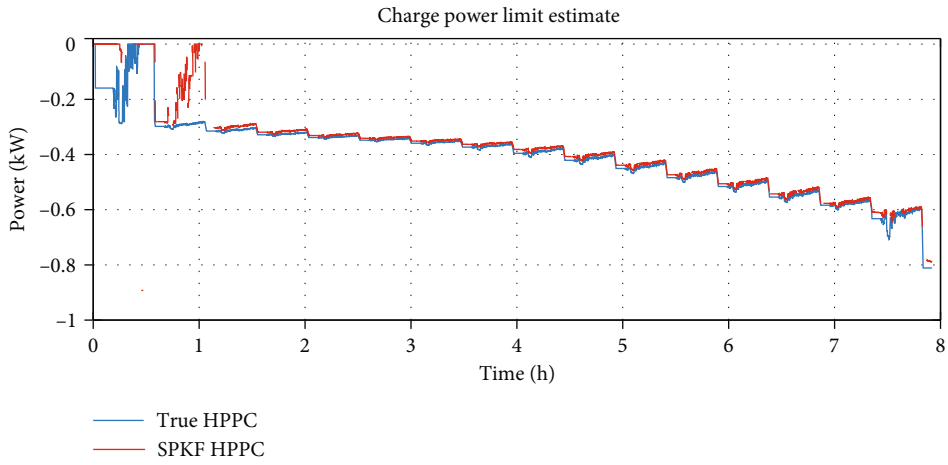

Figure 9: Charge power limit estimation using HPPC and SPKF HPPC.

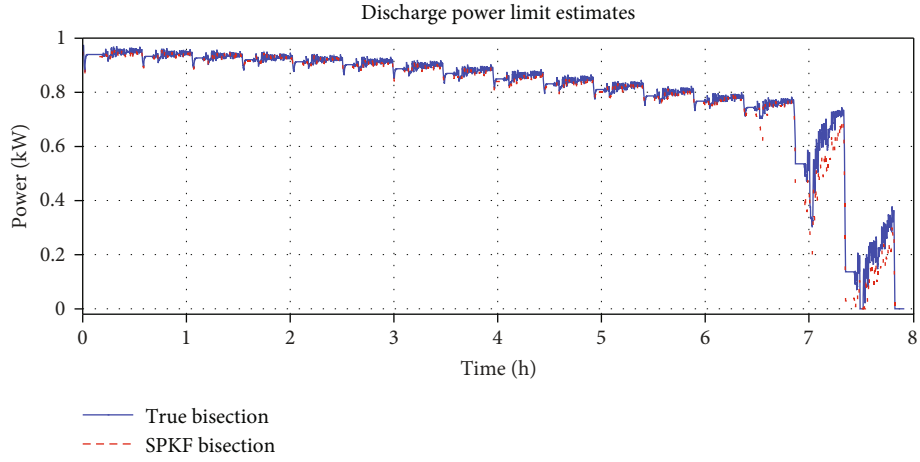

Figure 10: Power limit estimation during discharging using bisection method.

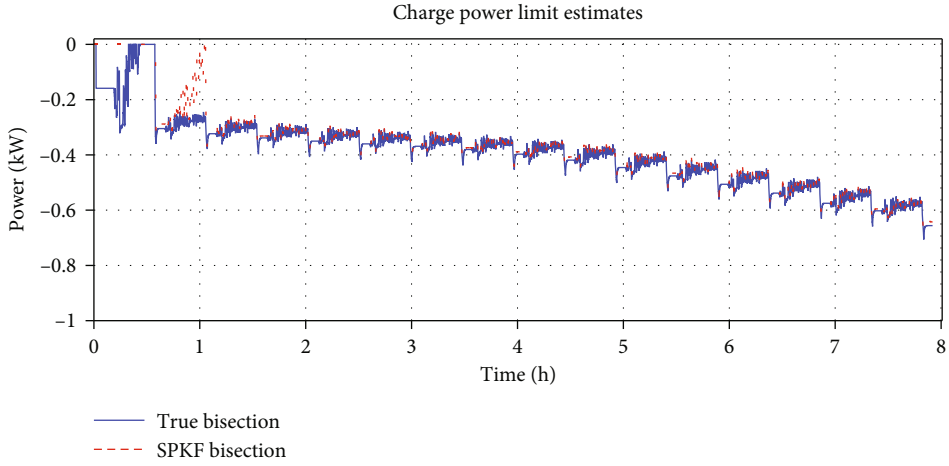

Figure 11: Power limit estimation during charging using bisection method.

The initial condition for cell was considered as 25°C and SOC% as 50%. The SOC was varied between 10% and 90%, voltage from 2.8 V to 4.3 V, and current from -200 A to 350 A. In bisection search, zero crossing was observed. The effective resistance values were calculated, and power limits were estimated for 8-hour duration. The power estimation techniques have been implemented through simulation studies carried out in Jupyter Notebook using Octave codes. The

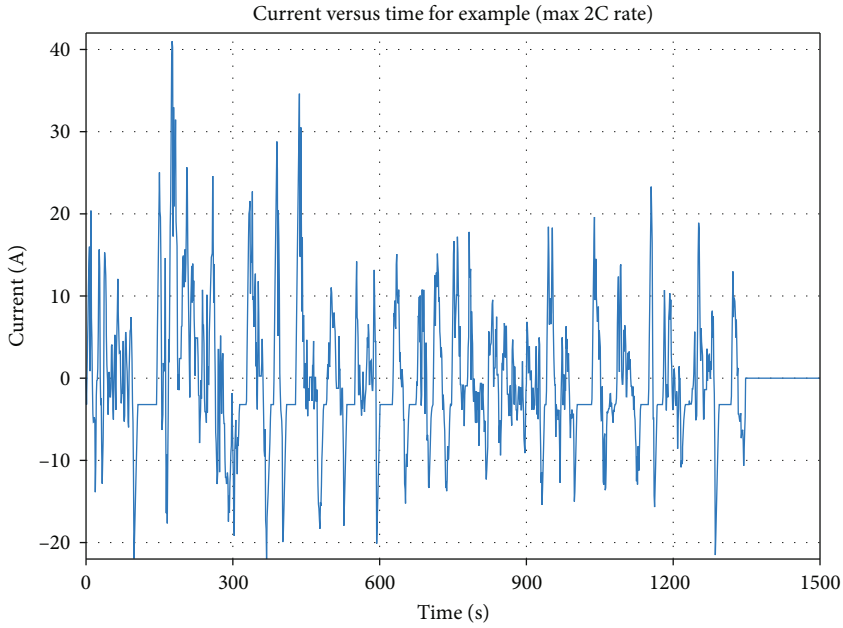

Figure 12: Reduced order model simulation for charge.

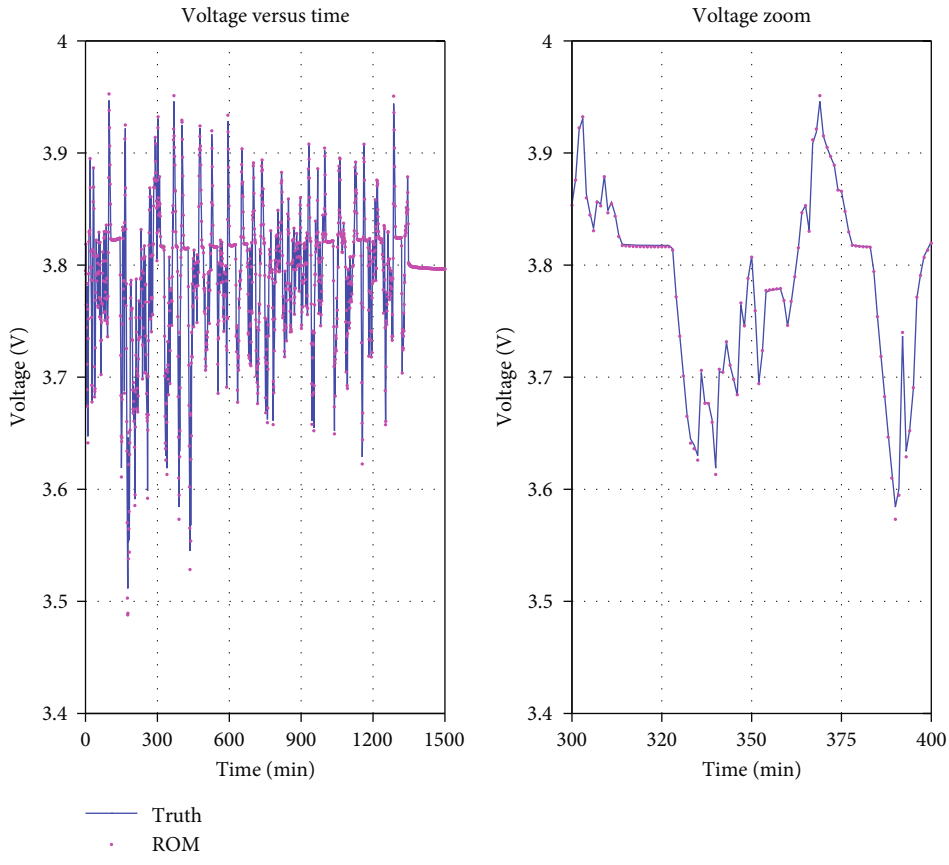

Figure 13: Reduced order model simulation for voltage plot.

experimental values, i.e., true values and the power estimation results obtained based on the simulation studies, are compared to check its validity. The results obtained from simulation studies and experimental values are discussed in the below section.

5. Results and Discussion

The experimental values and the results obtained from the simulation studies are described in this section. Figure 7

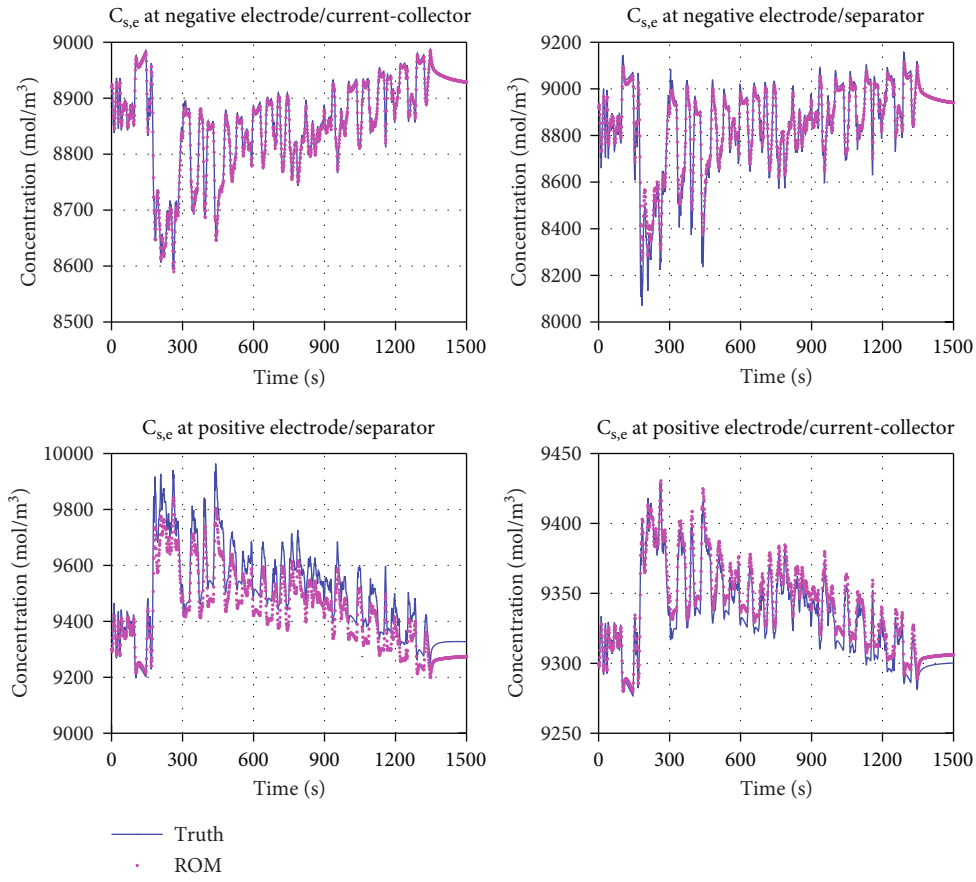

FIGURE 14: Reduced order model simulation for solid surface conc. at negative and positive electrodes.

shows how quickly a battery pack becomes unbalanced. Here, we simulated a battery pack having cell-to-cell variations. The purpose was to see how quickly we might expect the pack to become out of balance after discharging and charging for multiple cycles. Here, the batteries were simulated for the SOC% variation between 20% and 90% for discharging and charging conditions. It was simulated for 5 randomly selected battery packs, each having 100 cells for 20 discharge/charge cycles. A histogram of the relative frequency of end-of-charge SOC after the completion of 20 discharge/charge cycles is shown here in Figure 7. This helps in visualizing the spread of SOC values as well as their overall distribution after 20 cycles. The difference between minimum SOC and maximum SOC of all cells simulated over 20 cycles was also analysed, which were observed between 21.59% and 21.73%. The SOC spread in percent after 20 cycles is 0.15%.

HPPC power limit was obtained based on knowledge of true SOC and also based on an SOC estimate output by a sigma point Kalman filtering. In dataset, profiles of power versus time were demanded from a cell and the resulting data were used by an SPKF to estimate SOC. True SOC was used to calibrate the testing. Firstly, effective resistances were computed and then used in HPPC method. The obtained results are shown in Figure 8. The initial condition for cell was considered as 25°C and SOC% as 50%. The SOC was varied between 10% and 90%, voltage from 2.8 V to 4.3 V, and current from -200 A to 350 A. The effective resistances were obtained as 3.68 mΩ for charging and 3.70 mΩ for discharging. The power limit obtained for discharging is shown in Figure 8, and the power limit obtained for charging is shown in Figure 9. It can be seen that during discharging from 0 to 7 hours, maximum power can be around 0.9 kW to 0.8 kW, while in between 7 and 8 hours, power limit drops from 0.8 kW to 0 W. During charging, the power limit was observed as 0 to 0.2 kW for 0-1 hour, 0.2 to 0.4 kW for 1-5 hours, 0.4 to 0.5 kW for 5-7 hours, and 0.5 to 0.7 kW for 7-8 hours.

It can be said that, when the vehicle is running, it is consuming energy from the battery. Hence, battery gets slowly discharged. As the SOC% and terminal voltage for cells decrease, its ability for delivery maximum power get decreases. Similarly, when charging starts, then the SOC% and battery terminal voltage increase, so the ability to deliver maximum power increases with time. When the battery pack is fully charged, that is the time it can deliver maximum power. The negative sign denotes the opposite direction for the power flow.

We further analysed power limits using bisection method. A bisection search was implemented for a zero crossing (a root) of an arbitrary function between two limits. Here, we used bisection search to find a zero crossing

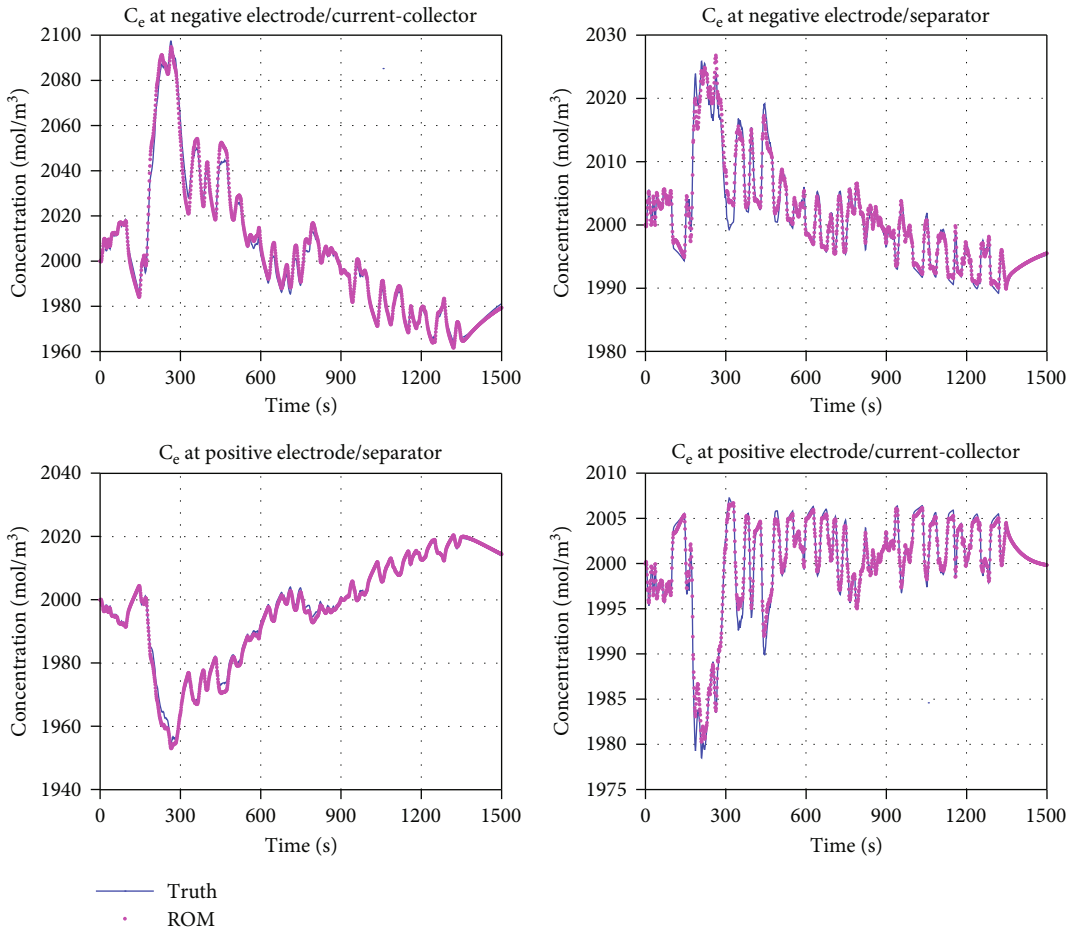

Figure 15: Reduced order model simulation for electrolyte conc. at negative and positive electrodes.

between -1 and 2 with tolerance of 10^{-5}. The zero crossing was obtained at -9.5×10^{-7}. The initial condition for the cell was considered as 25°C and SOC% as 50%. The voltage was obtained as 3.96 V after 10 seconds of discharge with 1 A current. Here, we have computed power limits for all points in time corresponding to a dynamic cell test. It uses the bisection method, first with ideal knowledge of cell state and then with SPKF estimated cell states. Bisection power estimation using true cell state as well as using SPKF was carried out for 28510 iterations. The power limit obtained for discharging using bisection method is shown in Figure 10, and the power limit obtained for charging using bisection method is shown in Figure 11. Here, also it can be seen that during discharging from 0 to 3 hours, maximum power can be around 0.9 kW, between 3 and 8 hours of power limit drops from 0.9 kW to 0.5 kW, while power limit drops from 0.5 kW to 0 W and no power after 8 hours. During charging, the power limit was observed as 0 to 0.3 kW for 0-1 hour, 0.3 to 0.4 kW for 1-5 hours, 0.4 to 0.6 kW for 5-7 hours, and 0.6 kW for 7-8 hours.

Further, we have carried out simulation studies using reduced order model (ROM) for charging and discharging conditions. This model was chosen as it gives faster results (similar to four resistor-capacitor equivalent-circuit model) then the earlier used model. We were also able to evaluate how well ROM predicts various intracellular electrochemical variables against their actual values at various cell sites. Figure 12 shows the current plot for 25 minutes, using max current at 2C rate. The voltages were also predicted for the same interval of 25 minutes using reduced order model. The true value of the voltage and the predicted voltage using ROM method are illustrated in Figure 13. It was observed that cell voltage varied between 3.48 V and 3.95 V.

Further, solid surface study was carried out for four subcellular regions which were obtained using reduced order method. These four locations were (a) negative electrode, at electrode/current-collector boundary, (b) negative electrode, at electrode/separator boundary, (c) positive electrode, at electrode/separator boundary, and (d) positive electrode, at electrode/current-collector boundary. The true value and the results obtained using ROM for the solid surface concentration at four mentioned locations are shown in Figure 14. The solid surface concentration at negative electrode/current collector varies from 8590 to 8990 mol/m^3, negative electrode/separator varies from 8050 to 9150 mol/m^3, positive electrode/separator varies from 9200 to 9980 mol/m^3, and positive electrode/current collector varies from 9275 to 9425 mol/m^3.

Next, we have analysed the electrolyte concentration at the above four mentioned locations in the cell. The true

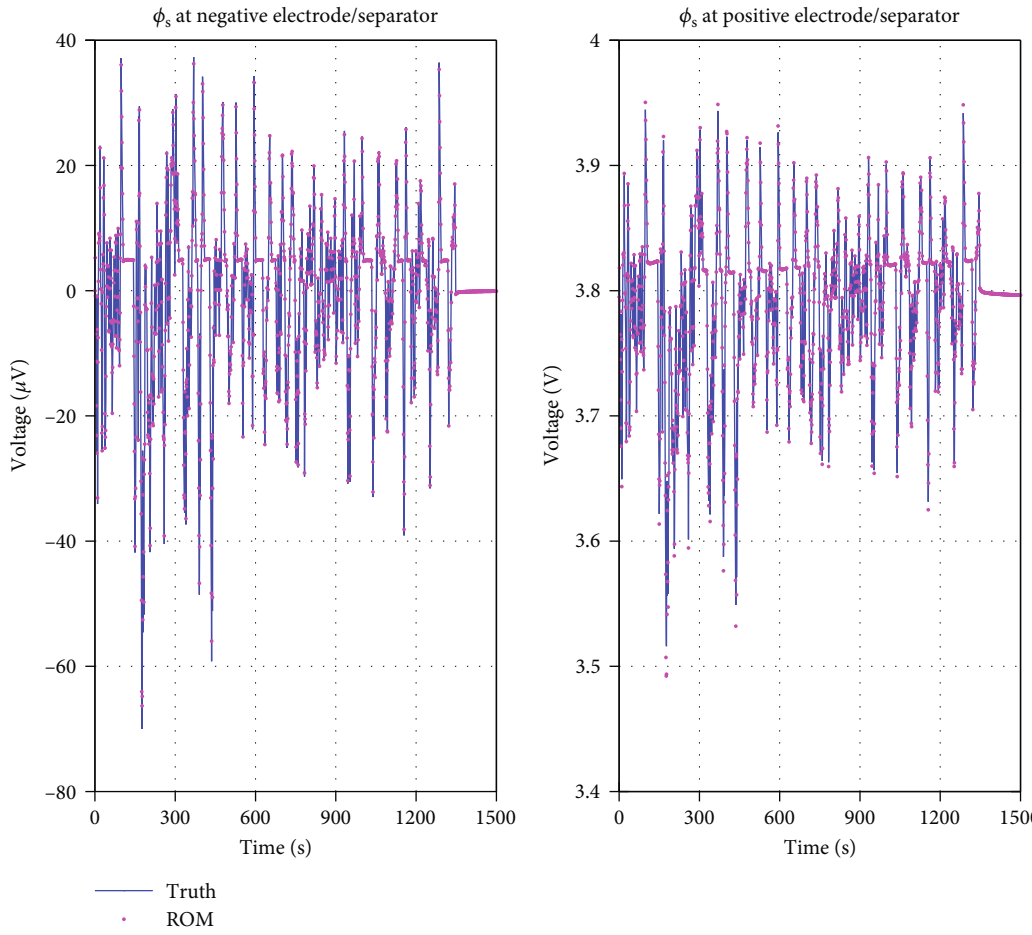

FIGURE 16: Reduced order model simulation for solid potential voltage at negative and positive electrodes.

value and the results obtained using ROM for the electrolyte concentration at four mentioned locations are shown in Figure 15. The electrolyte concentration at negative electrode/current collector varies from 1960 to 2096 mol/m^3, negative electrode/separator varies from 1988 to 2027 mol/m^3, positive electrode/separator varies from 1952 to 2022 mol/m^3, and positive electrode/current collector varies from 1978 to 2007 mol/m^3.

Next, we have attempted to plot solid potential. Solid potential is zero at negative electrode current collector and equal to cell voltage at positive-electrode current collector. The solid potential at the remaining two locations showed variations which were analysed and shown in Figure 16. Solid potential at negative electrode/separator was observed varying between -70 μV and 36 μV and at positive electrode/separator was observed varying between 3.49 V and 3.95 μV.

Next, we have analysed electrolyte potential at the four earlier mentioned locations in the cell. The true value and the results obtained using ROM for the electrolyte potential at four mentioned locations are shown in Figure 17. The final voltage estimation RMS error was carried out which was obtained as 1.76 mV. The electrolyte potential at negative electrode/current collector varies from -0.374 V to -0.298 V, negative electrode/separator varies from -0.454 V to -0.25 V, positive electrode/separator varies from -0.59 V to -0.23 V, and positive electrode/current collector varies from -0.52 V to -0.22 V.

We also analysed flux from solid to electrolyte. The true value and the results obtained using ROM for the flux from solid to electrolyte at the four mentioned locations are shown in Figure 18. The flux at negative electrode/current collector varies from -10 μmol/m^2/sec to 18 μmol/m^2/sec, negative electrode/separator varies from -37 μmol/m^2/sec to 72 μmol/m^2/sec, positive electrode/separator varies from -70 μmol/m^2/sec to 29 μmol/m^2/sec, and positive electrode/current collector varies from -11 μmol/m^2/sec to 6 μmol/m^2/sec.

Side-reaction rate due to solid electrolyte interphase (SEI) growth was also analysed. Figure 19 represents side-reaction rate due to SEI growth. Here, large negative values can be considered as bad (very fast side reaction), and values near zero can be considered as good (slow side reaction). It can be seen that side reaction rate is maximum when SOC is max, i.e., 100% and when *C*-rate is more, i.e., higher current.

In next section, we have shown the results for cell balancing. As mentioned earlier, in this study, we have used passive balancing techniques for balancing the cells. We have tuned the resistance values used in the switched-resistor

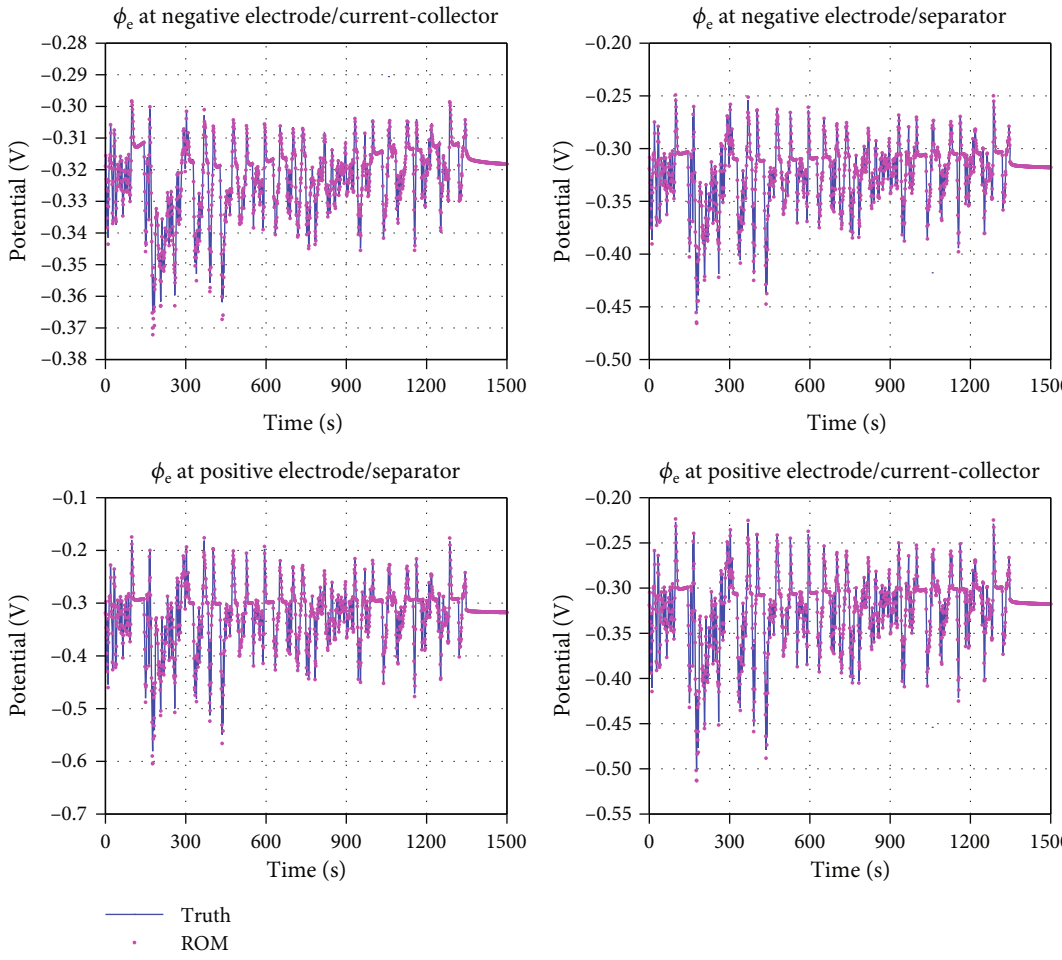

Figure 17: Reduced order model simulation for electrolyte potential at negative and positive electrodes.

passive balancing system, to obtain a better balancing. When the resistance value is too low, balancing power dissipated by the resistor is high. The total heat generated by all balancers in the pack will be high, resulting in a need for a bigger (and more expensive) thermal-management system. But the balancing is fast. When the larger (and more expensive) resistor and transistor components are used, balancing is slow, but heat generation is less. Hence, choosing the appropriate value for the balancing resistance is important.

Figure 20 shows an unbalanced battery pack, with individual SOC values. These cells have SOC% values between 87% and 95%. It consists of 100-cell battery pack having mismatched cells. This was achieved with more than 3,000 miles (around 5,000 km) of vehicle driving plus multiple battery pack charging events, all without balancing. Here, we have used different balancing resistance values for balancing the system. The balancing strategy is based on cell terminal voltage, and cells are balanced whenever their terminal voltage is more than 2 mV greater than the minimum terminal voltage of all 100 cells in the battery pack.

Maximum cell voltage is around 4.2 V. Cell power can be represented by V^2/r. Maximum power dissipated by all cells in a 100-cell battery pack occurs when 99 cells are above the minimum voltage. In this case, maximum pack power can be represented as $99\,V^2/r$. This information was useful in guessing the initial value of balancing resistance, which were further fine-tuned to get the best results, which are given in Table 2. Balancing process is explained through the flowchart given in Figure 21. Once balancing is completed, the obtained plots are represented in Figure 22.

From Table 2, it can be seen that, if 5 Ω resistor is used, it can balance the battery pack in less than 1 hour; however, 329.9058 W power will be lost. If 200 Ω resistor is used, it can balance the battery pack in less than 29.2375 hours, and the power loss will be only 8.2476 W. Hence, it can be said that, if the balancing resistance value is lower, the balancing is fast, but the balancing power is high which is getting wastages as heat. If the balancing resistance is high, the balancing is slow, but the balancing power is less. This switched-resistor-based balancing is inexpensive, compact, and easy to regulate and fabricate [72], in comparison to other techniques. Table 3 shows the reported results by the authors in [73], for cell balancing for three cells under study for the equalization time and energy loss. Table 4 shows the reported results for cell balancing for four-cell combination.

Figure 22 represents the status of the battery pack post balancing done with the help of 170 Ω resistor; in this case, individual cell balancing power was obtained as 0.0992 W, total balancing for the battery pack as 9.7031 W, and

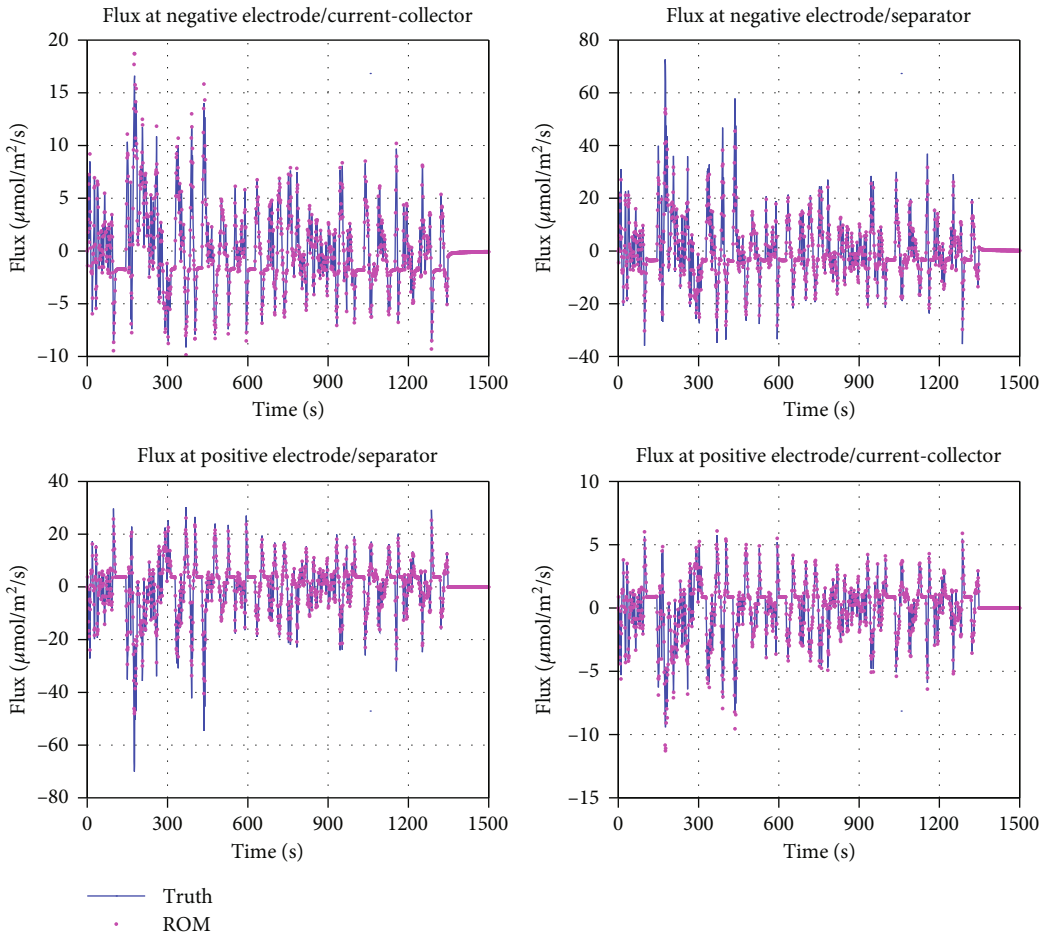

Figure 18: Reduced order model simulation for flux at negative and positive electrodes.

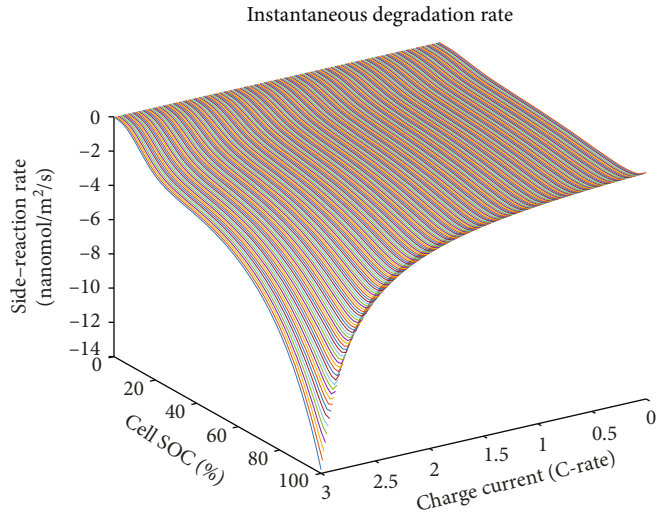

Figure 19: Side-reaction rate due to SEI growth.

balancing time as 24.8114 hours. At this stage, almost all the cells are balanced, with SOC around 87%. Terminal voltages of all cells came around 4.06 V.

It can be noted that the balancing power should be less than 10 W for efficient practical applications and for wider acceptance by the users. The individual cell's balancing power should be less than 0.1 W. Total balancing time should be less than 30 hours. Authors recommend the balancing with the 170 Ω resistor using this switched-resistor balancing technique, as it satisfies most preferred users

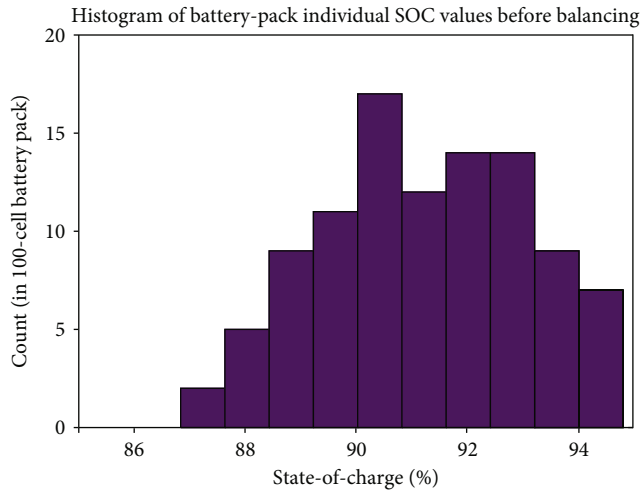

Figure 20: Histogram of battery pack individual SOC values before balancing.

Table 2: Balancing resistance, balancing power, and balancing time based on simulation study.

Sr. no.	Balancing resistance (Ω)	Cell balancing power (W)	Battery pack total balancing power (W)	Balancing time (hours)
1	5	3.3728	329.9058	0.7222
2	10	1.6864	164.9529	1.4466
3	20	0.8432	82.4765	2.8969
4	30	0.5621	54.9843	4.3481
5	40	0.4216	41.2382	5.8006
6	50	0.3373	32.9906	7.2544
7	100	0.1686	16.4953	14.5417
8	150	0.1124	10.9969	21.8686
9	160	0.1054	10.3096	23.3389
10	165	0.1022	9.9971	24.0747
11	170	0.0992	9.7031	24.8114
12	175	0.0964	9.4259	25.5478
13	180	0.0937	9.1641	26.2847
14	190	0.0888	8.6817	27.7603
15	200	0.0843	8.2476	29.2375

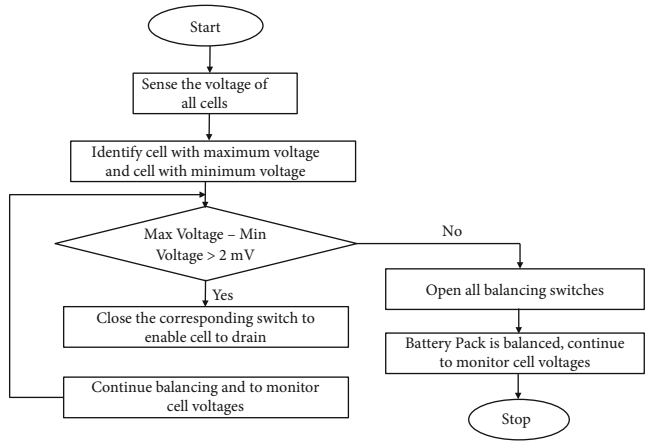

Figure 21: Flowchart representing proposed passive balancing approach.

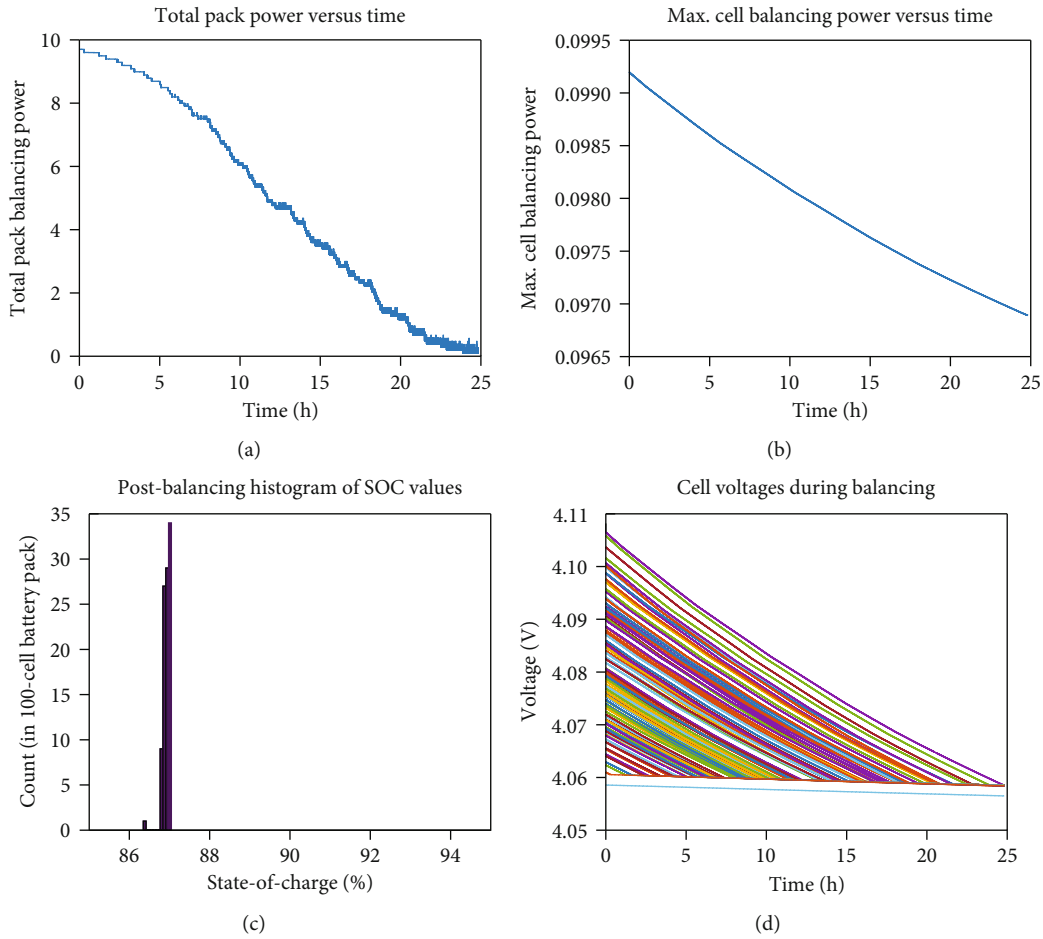

Figure 22: Battery pack status after balancing from switched-resistor passive balancing system: (a) total pack power versus time, (b) maximum cell balancing power versus time, (c) postbalancing histogram of SOC values, and (d) cell voltages during balancing.

Table 3: Balancing time and energy loss for three-cell pack balancing as reported in [73].

Cell voltage	Cells	Initial SOC	Passive cell balancing using switched shunt resistor			Active cell balancing using single switched capacitor		
			Final SOC	Equalization time (sec)	Energy loss (mWh)	Final SOC	Equalization time (sec)	Energy loss (mWh)
3.3 V	Cell 1	100%	60%	2200	7.1	94%	—	0.5 (in 12 hrs)
	Cell 2	90%	55%			90%		
	Cell 3	60%	60%			66%		
7.1 V	Cell 1	100%	65%	950	11.5	85%	40000	0.5
	Cell 2	90%	65%			85%		
	Cell 3	60%	60%			80%		

Table 4: Equalization details for four-cell battery bank as reported in [30, 74–76].

Equalizer	Component count	Equalization time (s)	Power loss (W)	Efficiency
Switched-inductor topology	6 MOSFETs, 3 inductors	16	6.22	85.87% [30]
Layer of inductor topology	6 MOSFETs, 3 inductors	15	6.99	88.1% [30, 74]
Single inductor topology	10 MOSFETs, 10 diodes, and 1 inductor	23	2.46	83.21% [75]
Single inductor architecture	2 MOSFETs, 5 SPDTs, and 1 inductor	22	4.43	84.9% [76]
Switched resistor	4 resistors	17.7	—	[30]

criteria. It can be said that this balancing technique can be effectively used for balancing cells in practical applications, in electric vehicles.

6. Conclusion

Constantly keeping tabs on individual lithium-ion cells, balancing and reliable operation of a lithium-ion battery pack is a major challenge. If these imbalances are not corrected, they will only get worse during repeated charge and discharge cycles. Battery SOC of each battery cell after 20 cycles was plotted to show though the simulation study, that how quickly SOC can diverge. By causing overvoltage and undervoltage cell situations, which will quickly damage and age the batteries and may cause overheating and catastrophic failure, this will reduce the performance of the battery pack. Even if the vehicle is stored for extended periods, balancing is required due to self-discharge. In the study, a switched-resistor passive balancing of Li-ion battery pack was proposed. The experimental data, simulation study, and the implementation of the passive balancing process of lithium-ion battery pack were the focus of this study. Current variation and cell voltage variation, solid surface concentration at electrodes, solid potential voltage, electrolyte concentration, electrolyte potential, and flux variations were studied at negative and positive electrodes. It was also observed that side reaction rate is maximum when SOC is maximum and *C*-rate is more. The power limits were estimated for charging and discharging conditions, using HPPC and bisection methods. It was observed that power limit increases after charging and decreases after discharging, based on the battery SOC% and terminal voltage. Maximum power was estimated as 0.9 kW for 0 to 1 hour during discharge. Maximum power was estimated as 0.5-0.7 kW during 7-8 hours of charging. Multiple iterations were performed to examine the effectiveness of the proposed balancing design. We executed the developed code for multiple discharge/charge profiles over many random battery packs, each containing 100 cells, under a variety of scenarios. The suggested balancing algorithms were used to identify the unbalanced cells, and switches were used to balance them. The outlier cells were identified and balanced which helps in boosting usable energy. Results obtained show that, if the balancing resistance value was lower, the balancing was fast, but the balancing power is high which is getting wastages as heat. If the balancing resistance was high, the balancing was slow, but the balancing power was less. Balancing of the given unbalanced pack was achieved with the help of 170 Ω balancing resistor, with individual cell balancing power as 0.09 W and total balancing power for the battery pack as 9.70 W in 24.81 hours. It helps in enhancing battery pack performance, increases the life cycle, and hence ensures a very safe operation during most challenging conditions. Hence, it can be stated that the balancing method is an essential technique for uninterruptible and reliable power supply from energy storage system in electrical vehicles. Further, cell balancing can be attempted with active balancing and using intelligent techniques.

Data Availability

No underlying data was collected or produced in this study.

Conflicts of Interest

The authors declare that they have no conflicts of interest.

Funding

We also acknowledge the "KLEF-2103040001" (S. Kumar) fellowship provided for the successful completion of the research work.

Acknowledgments

The article was supported by the International Research: SA/China Joint Research Programme 2021, with Reference No. BCSA210303588702 and Unique Grant No. 148770.

References

[1] April 2023, https://www.energy.gov/articles/history-electric-car.

[2] F. Un-Noor, S. Padmanaban, L. Mihet-Popa, M. N. Mollah, and E. Hossain, "A comprehensive study of key electric vehicle (EV) components, technologies, challenges, impacts, and future direction of development," *Energies*, vol. 10, no. 8, p. 1217, 2017.

[3] Q. Ouyang, Z. Han, C. Xu, and Z. Wang, "Cell balancing control for lithium-ion battery packs: a hierarchical optimal approach," *IEEE Transactions on Industrial Informatics*, vol. 16, pp. 5065–5075, 2019.

[4] V. Vardwaj, V. Vishakha, K. Jadoun, N. Jayalaksmi, and A. Agarwal, "Various methods used for battery balancing in electric vehicles: a comprehensive review," in *Proceedings of the 2020 International Conference on Power Electronics & IoT Applications in Renewable Energy and its Control (PARC)*, pp. 208–213, Mathura, Uttar Pradesh, India, 28–29 February, 2020.

[5] S.-R. Lee, B.-Y. Choi, M.-G. Kim, E.-J. Ha, and C.-Y. Won, "Battery balancing algorithm for serial multi-module UPS system," in *2014 IEEE Conference and Expo Transportation Electrification Asia-Pacific (ITEC Asia-Pacific)*, pp. 1–5, Beijing, China, 2014.

[6] J. B. Zhang, L. G. Lu, and Z. Li, "Key technologies and fundamental academic issues for traction battery system," *Journal of Automotive Safety and Energy*, vol. 3, no. 2, pp. 87–104, 2012.

[7] M. Einhorn, W. Roessler, and J. Fleig, "Improved performance of serially connected Li-ion batteries with active cell balancing in electric vehicles," *IEEE Transactions on Vehicular Technology*, vol. 60, no. 6, pp. 2448–2457, 2011.

[8] S. G. Xu, Q. S. Zhong, and R. J. Zhu, "Research of equalizing charge control strategy for power battery," *Electric Machines and Control*, vol. 16, pp. 62–65, 2012.

[9] A. G. Xu, S. J. Xie, and X. B. Liu, "Dynamic voltage equalization for series-connected ultracapacitors in EV/HEV applications," *IEEE Transactions Vehicular Technology*, vol. 58, no. 8, pp. 3981–3987, 2009.

[10] J. Cao, N. Schofield, and A. Emadi, "Battery balancing methods: A comprehensive review," in *In 2008 IEEE Vehicle*

Power and Propulsion Conference, pp. 1–6, Harbin, China, 2008.

[11] Y. Xing, E. W. M. Ma, K. L. Tsui, and M. Pecht, "Battery management systems in electric and hybrid vehicles," *Energies*, vol. 4, no. 11, pp. 1840–1857, 2011.

[12] S. Hemavathi, "Overview of cell balancing methods for Li-ion battery technology," *Energy Storage*, vol. 3, no. 2, article e203, 2021.

[13] A. Vezzini, "Lithium-ion battery management," in *Lithium-Ion Batteries Advance and Applications*, Elsevier, 2014.

[14] M. S. Yusof, S. F. Toha, N. A. Kamisan, N. N. W. N. Hashim, and M. A. Abdullah, "Battery cell balancing optimisation for battery management system," *IOP Conference Series: Materials Science and Engineering*, vol. 184, no. 1, article 012021, 2016.

[15] Z. C. Gao, C. S. Chin, W. D. Toh, J. Chiew, and J. Jia, "State-of-charge estimation and active cell pack balancing design of lithium battery power system for smart electric vehicle," *Journal of Advanced Transportation*, vol. 2017, Article ID 6510747, 14 pages, 2017.

[16] X. Wu, C. Hu, J. Du, and J. Sun, "Multistage CC-CV charge method for Li-ion battery," *Mathematical Problems in Engineering*, vol. 2015, Article ID 294793, 10 pages, 2015.

[17] B. S. Bhangu, P. Bentley, D. A. Stone, and C. M. Bingham, "Nonlinear observers for predicting state-of-charge and state-of-health of lead-acid batteries for hybrid-electric vehicles," *IEEE Transactions on Vehicular Technology*, vol. 54, no. 3, pp. 783–794, 2005.

[18] V. Chandola, A. Banerjee, and V. Kumar, "Anomaly detection for discrete sequences: a survey," *IEEE Transactions on Knowledge and Data Engineering*, vol. 24, no. 5, pp. 823–839, 2012.

[19] F. Angiulli and C. Pizzuti, "Outlier mining in large high-dimensional data sets," *IEEE Transactions on Knowledge and Data Engineering*, vol. 17, no. 2, pp. 203–215, 2005.

[20] Y. Lee, S. Jeon, J. Yun, and S. Bae, "Comparison of battery cell balancing methods," in *Proceedings of International Conference on Information and Convergence Technology for Smart Society (ICICTS '16)*, pp. 125-126, Vietnam, 2016.

[21] D. Andrea, *Battery management systems for large lithium-ion battery packs*, Artech House, 2010.

[22] M. Nawaz, J. Ahmed, and G. Abbas, "Energy-efficient battery management system for healthcare devices," *Journal of Energy Storage*, vol. 51, article 104358, 2022.

[23] N. Neil Samaddar, S. Kumar, and R. Jayapragash, "Passive cell balancing of Li-ion batteries used for automotive applications," *Journal of Physics: Conference Series*, vol. 1716, article 012005, 2020.

[24] M. Nawaz, J. Ahmed, and M. S. Khan, "Cell balancing techniques for Li-ion batteries in healthcare devices," in *2022 Global Conference on Wireless and Optical Technologies (GCWOT)*, pp. 1–7, Malaga, Spain, 2022.

[25] H. Bashir, A. Yaqoob, F. Kousar, W. Khalid, S. Akhtar, and W. Sultan, "A comprehensive review of Li-ion battery cell balancing techniques & implementation of adaptive passive cell balancing," in *2022 International Conference on Electrical Engineering and Sustainable Technologies (ICEEST)*, pp. 1–6, Lahore, Pakistan, 2022.

[26] B. Jiang, Y. Liu, X. Huang, and R. R. R. Prakash, "A new battery active balancing method with supercapacitor considering regeneration process," in *IECON 2020 The 46th Annual Conference of the IEEE Industrial Electronics Society*, pp. 2364–2369, Singapore, 2020.

[27] Y. Zhang and H. Zhu, "Intelligent cell balancing of Li-ion batteries: a particle swarm optimization methodProceedings of International Conference on Image, Vision and Intelligent Systems 2022 (ICIVIS 2022), Singapore.

[28] T. A. Abdul-jabbar, A. Kersten, A. Mashayekh, A. A. Obed, A. J. Abid, and M. Kuder, "Efficient battery cell balancing methods for low-voltage applications: a review," in *IEEE international conference in power engineering application (ICPEA)*, pp. 1–7, Shah Alam, Malaysia, 2022.

[29] U. R. Muduli, K. A. Jaafari, K. A. Hosani, R. K. Behera, R. R. Khusnutdinov, and A. R. Safin, "Cell balancing of li-ion battery pack with adaptive generalised extended state observers for electric vehicle applications," in *IEEE Energy Conversion Congress and Exposition (ECCE)*, pp. 143–147, Vancouver, BC, Canada, 2021.

[30] J. Carter, Z. Fan, and J. Cao, "Cell equalisation circuits: a review," *Journal of Power Sources*, vol. 448, article 227489, 2020.

[31] B. Jiang, *Active Cell Balancing Algorithms in Lithium-ion Battery, Master's Thesis in Science*, Chalmers University of Technology, Gothenburg, Sweden, 2020, https://odr.chalmers.se/server/api/core/bitstreams/d810c7c0-55d0-4dbb-ad63-90d083c0ed4b/content.

[32] E. Cılız, *Centra-Modular and Reconfigurable Battery Management System Design for Lithium-Ion Battery Packs*, Altinbas University, Istambul, 2022.

[33] X. Yan, J. Nie, Z. Ma, and H. Ma, "Development status of balanced technology of battery management system of electric vehicle," in *Advanced Manufacturing and Automation IX*Springer, Singapore.

[34] N. Nuratma, S. Nordin, M. I. F. Romli, L. H. Fang, M. Z. Aihsan, and M. S. Saidon, "Review article: Voltage balancing method for battery and supercapacitor as energy storage," *Journal of Advanced Research in Applied Sciences and Engineering Technology*, vol. 29, no. 3, pp. 235–250.

[35] J. P. D. Faria, A. C. G. M. Fernandes, J. A. N. Pombo, M. R. A. Calado, and S. J. P. S. Mariano, "Supercapacitors voltage balancing methods: a comprehensive review," in *2022 IEEE International Conference on Environment and Electrical Engineering and 2022 IEEE Industrial and Commercial Power Systems Europe (EEEIC/I&CPS Europe)*, pp. 1–7, Prague, Czech Republic, 2022.

[36] F. Jiang, C. Jin, H. Liao et al., "An artificial potential field-based lithium-ion battery SOC equilibrium method in electric vehicles," *IFAC-PapersOnLine*, vol. 53, no. 2, pp. 12682–12687, 2020.

[37] A. Alvarez-Diazcomas, A. A. Estevez-Ben, J. Rodriguez-Resendiz, M.-A. Martinez-Prado, R. V. Carrillo-Serrano, and S. Thenozhi, "A review of battery equalizer circuits for electric vehicle applications," *Energies*, vol. 13, no. 21, p. 5688, 2020.

[38] A.-M. Petri, *Theoretical and Experimental Research of the Propulsion System for an Electric Vehicle, [Ph.D. Thesis]*, Electronics, Telecommunications, and Information Technology, Technical University of Cluj-Napoca, 2023.

[39] W. Bartek, *Passive and Active Battery Balancing Methods Implemented on Second Use Lithium-ion Batteries*, Grand Valley State University, 2020.

[40] A. Alvarez-Diazcomas, A. A. Estévez-Bén, J. Rodríguez-Reséndiz, M.-A. Martínez-Prado, and J. D. Mendiola-Santíbañez, "A novel RC-based architecture for cell equalization in electric vehicles," *Energies*, vol. 13, no. 9, p. 2349, 2020.

[41] H. Liao, F. Jiang, C. Jin et al., "Lithium-ion battery SoC equilibrium: an artificial potential field-based method," *Energies*, vol. 13, no. 21, p. 5691, 2020.

[42] A. Farzan Moghaddam and A. Van den Bossche, "A Ćuk converter cell balancing technique by using coupled inductors for lithium-based batteries," *Energies*, vol. 12, no. 15, p. 2881, 2019.

[43] S. Narayanaswamy, S. Steinhorst, M. Lukasiewycz, M. Kauer, and S. Chakraborty, "Optimal dimensioning and control of active cell balancing architectures," *IEEE Transactions on Vehicular Technology*, vol. 68, no. 10, pp. 9632–9646, 2019.

[44] A. C. Fernandes and G. Marques, *Review on Supercapacitors: from Mathematical Modeling Techniques to their Integration as Electrical Energy Storage Devices*, Dissertation for obtaining the Master's Degree in Electrical and Computer Engineering, University of Beira Interior, Portugal, 2022, https://ubibliorum.ubi.pt/handle/10400.6/13083.

[45] A. Farzan Moghaddam and A. Van den Bossche, "A smart high-voltage cell detecting and equalizing circuit for LiFePO4 batteries in electric vehicles," *Applied Sciences*, vol. 9, no. 24, p. 5391, 2019.

[46] A. Jeyashree and L. Ashok Kumar, "Review on battery management system for electric vehicle application," in *Proceedings of the First International Conference on Combinatorial and Optimization, ICCAP 2021*, Chennai, India, December 2021.

[47] B. Wang, F. Qin, X. Zhao, X. Ni, and D. Xuan, "Equalization of series connected lithium-ion batteries based on back propagation neural network and fuzzy logic control," *International Journal of Energy Research*, vol. 44, no. 6, pp. 4812–4826, 2020.

[48] Y. Ma, P. Duan, Y. Sun, and H. Chen, "Equalization of lithium-ion battery pack based on fuzzy logic control in electric vehicle," *IEEE Transactions on Industrial Electronics*, vol. 65, no. 8, pp. 6762–6771, 2018.

[49] N. Nguyen, S. K. Oruganti, K. Na, and F. Bien, "An adaptive backward control battery equalization system for serially connected lithium-ion battery packs," *IEEE Transactions on Vehicular Technology*, vol. 63, no. 8, pp. 3651–3660, 2014.

[50] L. McCurlie, M. Preindl, and A. Emadi, "Fast model predictive control for redistributive lithium-ion battery balancing," *IEEE Transactions on Industrial Electronics*, vol. 64, no. 2, pp. 1350–1357, 2017.

[51] J. Liu, Y. Chen, and H. K. Fathy, "Nonlinear model-predictive optimal control of an active cell-to-cell lithium- ion battery pack balancing circuit," *IFAC-Papers Online*, vol. 50, no. 1, pp. 14483–14488, 2017.

[52] S. Zhang, L. Yang, X. Zhao, and J. Qiang, "A GA optimization for lithium-ion battery equalization based on SOC estimation by NN and FLC," *International Journal of Electrical Power & Energy Systems*, vol. 73, pp. 318–328, 2015.

[53] J. Sun, C. Zhu, R. Lu, K. Song, and G. Wei, "Development of an optimized algorithm for bidirectional equalization in lithium-ion batteries," *Journal of Power Electronics*, vol. 15, no. 3, pp. 775–785, 2015.

[54] Z. Liu, X. Liu, J. Han, and W. Yang, "An optimization algorithm for equalization scheme of series-connected energy storage cells," in *Proceedings of the IEEE Transportation Electrification Conference and Expo, Asia-Pacific (ITEC Asia-Pacific)*, pp. 1–6, Harbin, China, 2017b.

[55] G. Krishna and S. Prabhaharan, "Smart battery management system with active cell balancing," *Journal of Science and Technology*, vol. 8, no. 19, pp. 1–6, 2015.

[56] C. Piao, Z. Wang, J. Cao, W. Zhang, and S. Lu, "Lithium-ion battery cell-balancing algorithm for battery management system based on real-time outlier detection," *Mathematical Problems in Engineering*, vol. 2015, Article ID 168529, 12 pages, 2015.

[57] R. Sugathan, S. Ananda, V. Ramdas, P. Satyanarayana, M. Sankaran, and R. S. Ekkundi, "Worst case circuit analysis of a new balancing circuit for spacecraft application," in *Paper presented at: International Conference on Power and Advanced Control Engineering*, pp. 327–332, Bengaluru, India, 2015.

[58] M. Daowd, N. Omar, P. Van Den Bossche, and J. Van Mierlo, "Passive and active battery balancing comparison based on MATLAB simulation," in *Paper presented at: IEEE Vehicle Power and Propulsion Conference*, pp. 1–7, Chicago, IL, USA, 2011.

[59] S. W. Moore and P. J. Schneider, *A review of cell equalization methods for lithium ion and lithium polymer battery systems*, Society of Automotive Engineers, 2001.

[60] E. Loniza, J. A. Situmorang, D. D. A. Kusuma, A. I. Cahyadi, and O. Wahyunggoro, "Passive balancing of battery lithium polymer using shunt resistor circuit methodvol. 1755, AIP Conference Proceedings AIP Publishing LLC.

[61] M. Einhorn, F. Valerio Conte, and J. Fleig, "Improving of active cell balancing by equalizing the cell energy instead of the cell voltage," *World Electric Vehicle Journal*, vol. 4, no. 2, pp. 400–404, 2010.

[62] Z. Zhang, H. Gui, D. Gu, Y. Yang, and X. Ren, "A hierarchical active balancing architecture for lithium-ion batteries," *IEEE Transactions on Power Electronics*, vol. 32, no. 4, pp. 2757–2768, 2017.

[63] X. Cui, W. Shen, Y. Zhang, C. Hu, and J. Zheng, "Novel active $LiFePO_4$ battery balancing method based on chargeable and dischargeable capacity," *Computers and Chemical Engineering*, vol. 97, pp. 27–35, 2017.

[64] M. Gokdag and M. Akbaba, "An active battery cell balancing topology without using external energy storage elements," in *Paper presented at: 6th International Conference on Modeling, Simulation and Applied Optimization*, pp. 4–8, Istanbul, Turkey, 2015.

[65] G.-H. Min and J.-I. Ha, "Active cell balancing algorithm for serially connected Li-ion batteries based on power to energy ratio," in *2017 IEEE Energy Conversion Congress and Exposition (ECCE*, pp. 2748–2753, Cincinnati, OH, USA, 2017.

[66] W. Diao, N. Xue, V. Bhattacharjee, J. Jiang, O. Karabasoglu, and M. Pecht, "Active battery cell equalization based on residual available energy maximization," *Applied Energy*, vol. 210, pp. 690–698, 2018.

[67] J. Gallardo-Lozano, E. Romero-Cadaval, M. I. Milanes-Montero, and M. A. Guerrero-Martinez, "A novel active battery equalization control with on-line unhealthy cell detection and cell change decision," *Journal of Power Sources*, vol. 299, pp. 356–370, 2015.

[68] M. J. Isaacson, R. P. Hollandsworth, P. J. Giampaoli, F. A. Linkowsky, A. Salim, and V. L. Teofilo, "Advanced lithium ion battery charger," in *Fifteenth Annual Battery Conference on Applications and Advances (Cat. No.00TH8490)*, pp. 193–198, Long Beach, CA, USA, Jan. 2000.

[69] J. Xu, X. Mei, and J. Wang, "A high power low-cost balancing system for battery strings," *Energy Procedia*, vol. 158, pp. 2948–2953, 2019.

[70] S. R. Dos Santos, J. P. Fracarolli, A. Y. Narita et al., "Dissipative lithium ion cell balancing by recharge control and detection of

outliers for energy optimization and heat reduction," in *IECON 2018 44th Annual Conference of the IEEE Industrial Electronics Society*, pp. 5038–5043, Washington, DC, USA, 2018.

[71] T. A. Stuart and W. Zhu, "Fast equalization for large lithium ion batteries," *IEEE Aerospace and Electronic Systems Magazine*, vol. 24, no. 7, pp. 27–31, 2009.

[72] A. Ivan, "Modeling and control of a phase-shifted full-bridge converter for a LiFePO4 battery charger," *Electronics*, vol. 10, no. 21, p. 2568, 2021.

[73] A. Khanal, A. Timilsina, B. Paudyal, and S. Ghimire, "Comparative analysis of cell balancing topologies in battery management systems," in *Proceedings of the IOE Graduate Conference*, pp. 845–851, Lisbon, Portugal, May 2019.

[74] M. Y. Kim, J. W. Kim, C. H. Kim, S. Y. Cho, and G. W. Moon, "Automatic charge equalization circuit based on regulated voltage source for series connected lithium-ion batteries," in *Proceedings of the 8th International Conference on Power Electronics-ECCE Asia*, pp. 2248–2255, Jeju, Korea, 30 May–3 June 2011.

[75] S. Goodarzi, R. Beiranvand, S. M. Mousavi, and M. Mohamadian, "A new algorithm for increasing balancing speed of switchedcapacitor lithium-ion battery cell equalizers," in *Proceedings of the 6th Power Electronics, Drive Systems & Technologies Conference (PEDSTC2015)*, pp. 292–297, Tehran, Iran, 3–4 February 2015.

[76] A. Alvarez-Diazcomas, J. Rodríguez-Reséndiz, and R. V. Carrillo-Serrano, "An improved battery equalizer with reduced number of components applied to electric vehicles," *Batteries*, vol. 9, no. 2, p. 65, 2023.